OIKOS 89: 137–145. Copenhagen 2000

Patterns of spread in insect-pathogen systems: the importance of pathogen dispersal

Andrew White, Allan D. Watt, Rosie S. Hails and Sue E. Hartley

White, A., Watt, A. D., Hails, R. S. and Hartley, S. E. 2000. Patterns of spread in insect-pathogen systems: the importance of pathogen dispersal. – Oikos 89: 137–145.

A general model of insect-pathogen dynamics is presented which includes explicit host and pathogen dispersal. Four distinctive, wave-like, patterns of dispersal are produced which can be categorised by two universal parameters – the speed of advance, and the position of the leading edge, of the wave of dispersal of the host relative to that of the disease. These patterns are (1) the pathogen becomes extinct, allowing the host to disperse at the carrying capacity across the land surface, (2) the host disperses more rapidly than the pathogen, producing host densities at the carrying capacity in a region behind the leading edge of the wave, with these densities reduced due to interaction with the pathogen in the wave interior, (3) the host and pathogen disperse at the same speed but the leading edge of the host extends beyond that of the pathogen, allowing the host to reach 'high' density at the leading edge only, and (4) the host and pathogen disperse at the same speed but the leading edge of the pathogen extends beyond that of the host, producing 'low' density host dispersal across the land surface. A biological description explaining the causes of these patterns has important consequences regarding the use of pathogens for biological control of insect pests.

The model is modified to represent a specific insect-pathogen system, the winter moth, *Operophtera brumata*, and its nuclear polyhedrosis virus. The same patterns, categorised by the same universal parameters, are observed. Thus, it is suggested that the strength of infection and the relative dispersal rates of the host and pathogen are influential in determining the patterns of host outbreaks observed in this insect.

A. White, Inst. of Terrestrial Ecology, Bush Estate, Midlothian, UK EH26 0QB (present address: Dept of Mathematics, Heriot-Watt Univ., Edinburgh, UK EH14 4AS [awhite@ite.ac.uk]). – A. D. Watt and S. E. Hartley, Inst. of Terrestrial Ecology, Hill of Brathens, Glassel, Banchory, Kincardineshire, UK AB31 4BY. – R. S. Hails, Inst. of Virology and Environmental Microbiology, Mansfield Road, Oxford, UK OX1 3SR.

The use of pathogens to control insect pests is becoming increasingly popular. Technical advances have allowed pathogens to be isolated more readily and administered more effectively. Also, pathogens are efficient at targeting specific species without harming natural enemies or entering the food chain and are therefore perceived as more ecological than other control methods (i.e. chemical insecticides). Experiments (Bird and Elgee 1957, Bird and Birk 1961, Stairs 1965, Young 1974, Entwistle et al. 1983, Shepherd et al. 1984, Otvos et al. 1987a, b) conducted to assess the effects of pathogens on insect pests are in broad agreement that the pathogen can dramatically reduce the population density of the insect pest, its controlling effects on the population can continue over many seasons, and its spread is invariably observed beyond the region of introduction. Although such comments are common, these studies lack detailed descriptions of the patterns of dispersal, being concerned more with the mechanisms of dispersal or the effectiveness of the pathogen as a biological control agent. Consequently, most efforts to explain the patterns of disease spread are limited to lists of the possible dispersal agents of the pathogen (Table 1).

Accepted 30 July 1999

ISSN 0030-1299

An exception is the study by Entwistle et al. (1983) on the spread of nuclear polyhedrosis virus in *Gilpinia hercyniae* and hence their observations and interpretations have been widely accepted as portraying the expected pattern of disease dispersal in insects. They report that a wave-like pattern will develop, spreading the disease away from its initial point of introduction. Later, this waveform is lost and any pattern is less coherent, which they explain as the interaction between multiple waves of infection, and call the interference phase.

Due to the lack of detail in empirical studies, theoretical models have become necessary tools to investigate the patterns of spread in host-pathogen systems. These studies commonly use generalised model formulations (Dwyer 1992, 1994, Dwyer and Elkinton 1995, White et al. 1999) but have highlighted the possibility of a travelling wave of infection that corresponds well with the initial patterns of spread reported by Entwistle et al. (1983).

By including additional biological realism to general models, White et al. (1999) suggested that a single wave of infection may be the most likely cause of all patterns of disease dispersal in host-pathogen systems such as Entwistle et al.'s (1983), thereby challenging the existence of the so-called interference phase. Hence, theoretical models have provided invaluable insight into the possible causes of disease spread in host-pathogen systems. The theoretical analysis to date however has concentrated on one dispersal mechanism for the disease only; namely the movement of infected hosts. Field studies suggest that there is a range of possible dispersal agents (Table 1) and that these may be crucial in determining the behaviour of the system. Indeed, Dwyer and Elkinton (1995) suggest mechanical vectoring of disease by a parasitoid fly, above dispersal via larval movement, may be responsible for disease spread in gypsy moth (*Lymantria dispar*). Thus, there is a need to extend the theoretical analysis to examine the behaviour that can result from such alternative disease dispersal mechanisms.

Table 1. Reported mechanisms of pathogen dispersal. All but the movement of infected larvae can be approximated by the diffusion of pathogen particles.

Disease dispersal mechanism	Reference
Movement of infected larvae	Dwyer 1992, Dwyer and Elkinton 1995
Infection produced by contaminated vector contact with host.	
Dispersal by	
adult host	Bird and Elgee 1957, Young 1974, Entwistle et al. 1983
predators	Entwistle et al. 1983
parasites	Stairs 1965
Vector contamination of foliage (i.e. excretion of pathogen particles) which are subsequently consumed by hosts.	
Dispersal by	
adult host	Young 1974, Entwistle et al. 1983
predators	Entwistle et al. 1983

In this study, spatial interactions are modelled by extending the well-established representation of host-pathogen systems in which the pathogen is assumed to be 'free-living' (Anderson and May 1981, Bowers et al. 1993) to additionally include dispersal by virus carrying agents as well as by host movement. The range of possible spatial behaviour will be explored while assessing the importance of the different dispersal mechanisms. The results are presented in terms of general, but distinct, spatial patterns, and a biological description exploring the causes of the patterns and highlighting their significance for the population dynamics and the biological control of insect pests is presented.

The model

The host-pathogen interactions are described by a reaction-diffusion model, combining an interspecific interaction (i.e. the 'reaction kinetics', to describe the interplay between host and pathogen) with diffusive movement of the host and pathogen. The reaction kinetics are represented by Anderson and May's (1981) model G, but with the inclusion of a density-dependent term which models the effect of resource limitation on the host (Bowers et al. 1993). Such an approach has become the cornerstone from which such spatial models have been developed (Dwyer 1994, Dwyer and Elkinton 1995, White et al. 1999). The approach describes the behaviour of three classes: the density of healthy hosts, X, the density of infected hosts, Y, and the density of free pathogen particles, W. Previously the spatial effect has been included by adding diffusion terms to the healthy and infected host classes (Dwyer 1994, White et al. 1999), representing dispersal by host movement only. To represent the dispersal of pathogen particles by other mechanisms, we will additionally add a diffusion term to the pathogen class. Here, we recognise that the pathogen particles themselves cannot disperse but assume that movement by pathogen-bearing agents (e.g. through the faeces of birds or animals that consumed either the particles directly or infected larvae; from individuals who spread the pathogen by contact; or by what may be considered passive diffusion such as dispersal by wind or rain) occurs at a rate proportional to the number of particles at a particular location. Thus, the host-pathogen model consists of the following three partial differential equations (PDEs):

$$\frac{\partial X}{\partial t} = a(X+Y)(1-q(X+Y)) - bX - vXW + D_X\frac{\partial^2 X}{\partial x^2},$$
$$\frac{\partial Y}{\partial t} = vXW - (b+\alpha)Y + D_Y\frac{\partial^2 Y}{\partial x^2}, \qquad (1)$$
$$\frac{\partial W}{\partial t} = \lambda Y - (\mu + v(X+Y))W + D_W\frac{\partial^2 W}{\partial x^2}.$$

This system of equations models the dynamics of a host and pathogen over space, x and time, t. The parameters a and b represent the intrinsic birth and death rate of the host, respectively; α is the pathogenicity, that is the host death rate in excess of b, attributable to the pathogen; v is the transmission efficiency between the free-living pathogen stages and the host; λ is the rate at which free-living stages are produced by the host and μ is the decay rate of these stages; q is an intraspecific competition coefficient related to the carrying capacity, K, by $K = (a-b)/aq$. D_X, D_Y and D_W represent the diffusion coefficients of healthy hosts, infected hosts and the pathogen particles, respectively.

This representation is coupled with boundary conditions expressing the fact that individuals do not leave the region of interest (described to be $-L < x < L$), and given by:

$$\left.\frac{\partial X}{\partial x}\right|_{x=-L} = \left.\frac{\partial Y}{\partial x}\right|_{x=-L} = \left.\frac{\partial W}{\partial x}\right|_{x=-L} = \left.\frac{\partial X}{\partial x}\right|_{x=L} = \left.\frac{\partial Y}{\partial x}\right|_{x=L} = \left.\frac{\partial W}{\partial x}\right|_{x=L} = 0. \qquad (2)$$

The initial conditions assume that a number of susceptible hosts and pathogen particles invade at $x = 0$, at time $t = 0$. The model is run for a period $5t$. These initial conditions are chosen as they provide the most clarity in the observed patterns of host and pathogen spread. However, the same patterns of spread evolve if the host and pathogen are introduced at different points or if the pathogen is introduced across the entire landscape. (The significance and interpretation of this generality to initial condition will be discussed later.)

Results

Non-spatial model: D_X, D_Y and $D_W = 0$

Before analysing the effect of dispersal it is important to assess the behaviour of the reaction dynamics (i.e. eq. 1 with D_X, D_Y and $D_W = 0$), as they play an important role in determining the temporal and spatial behaviour (White et al. 1999). The full analysis of the reaction component of the model has been conducted elsewhere (Bowers et al. 1993) and so will not be repeated here. However, a summary of the results is as follows:

There are three biologically relevant (i.e. non-negative population density) equilibrium points: the origin

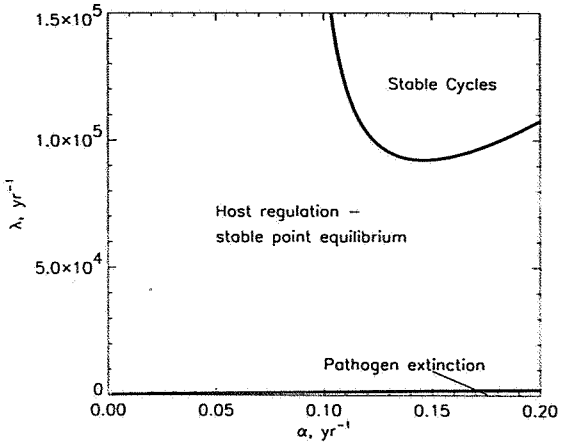

Fig. 1. The λ-α parameter space portrait detailing where different dynamic behaviour occurs in the general model (eq. 1) when the diffusion coefficients are set to zero. Here, $a = 0.05$ d^{-1}, $b = 0.025$ d^{-1}, $\mu = 0.01$ d^{-1}, $K = 100$ m^{-2}, $v = 1 \times 10^{-8}$ m^2 d^{-1}, $D_X = D_Y = D_W = 0$.

$(X, Y, W) = (0, 0, 0)$, the disease-free equilibrium $(K, 0, 0)$ and a coexistence equilibrium (X^*, Y^*, W^*). A stability analysis of these equilibria shows that the origin is always unstable, the disease-free equilibrium is stable if inequality (3) (below) is reversed and the coexistence equilibrium is stable or replaced by stable cycles around the coexistence equilibrium if:

$$\lambda > \Phi \quad \text{where} \quad \Phi = (\alpha + b)\left(1 + \frac{\mu}{vK}\right). \qquad (3)$$

Hence, the dynamics of this non-spatial model are qualitatively different in different regions of parameter space (Fig. 1). For details of how the boundary between coexistence and cycles is calculated see Bowers et al. (1993). In the spatial results below the parameters are chosen such that when $\lambda > \Phi$ the temporal model would produce a stable coexistence solution.

Spatial model

To enable the classification of the results for the spatial model it is useful to make two definitions.

1. Wave speed: u_X, u_Y and u_W are defined as the speed of the wave of healthy host, infected hosts and pathogen particle respectively. They are calculated by dividing the distance the wave has moved over the period $4t$ to $5t$ by t.
2. Leading edge: this refers to the leading edge of the wave and is defined as the furthest point from the region of introduction of host and pathogen at time $5t$ at which the density is greater than $X^*/10$, $Y^*/10$ or $W^*/10$ for the leading edge of healthy hosts l_X, infected hosts l_Y and pathogen particles l_W, respectively.

Table 2. Details of the wave speed and position of the leading edge of the host and pathogen for different values of the diffusion coefficients. The remaining parameters are fixed as $a = 0.05\ d^{-1}$, $b = 0.025\ d^{-1}$, $\alpha = 0.05\ d^{-1}$, $\lambda = 1.0 \times 10^4\ d^{-1}$, $\mu = 0.01\ d^{-1}$, $K = 100\ m^{-2}$ and A. $v = 1.0 \times 10^{-10}\ m^2\ d^{-1}$ and B. $v = 1.0 \times 10^{-8}\ m^2\ d^{-1}$. The type of behaviour (with reference to the result section) is displayed in parentheses.

Diffusion coefficient, $m^2\ d^{-1}$	Wave speed, $m\ d^{-1}$			Position of the leading edge, m		
	u_X	u_Y	u_W	l_X	l_Y	l_W
A. $\lambda<\Phi$, $D_X = 0.01$, $D_W = 0$						
(1) $D_Y = 0.01$	0.034	0	0	169	0	0
B. $\lambda>\Phi$, $D_X = 0.01$, $D_W = 0$						
(2) $D_Y = 0.002$	0.034	0.025	0.025	169	119	122
(2) $D_Y = 0.004$	0.034	0.032	0.032	169	143	147
(3) $D_Y = 0.006$	0.034	0.034	0.034	169	146	160
(3) $D_Y = 0.01$	0.034	0.034	0.034	169	161	165
(3) $D_Y = 0.02$	0.034	0.034	0.034	169	163	167
(4) $D_Y = 0.1$	0.038	0.038	0.038	189	186	198
(4) $D_Y = 0.5$	0.071	0.071	0.071	351	346	373
A. $\lambda<\Phi$, $D_X = 0.01$, $D_Y = 0$						
(1) $D_W = 0.01$	0.034	0	0	169	0	0
B. $\lambda>\Phi$, $D_X = 0.01$, $D_Y = 0$						
(2) $D_W = 0.002$	0.034	0.029	0.029	169	137	141
(2) $D_W = 0.003$	0.034	0.032	0.032	169	151	156
(3) $D_W = 0.004$	0.034	0.034	0.034	169	158	162
(3) $D_W = 0.01$	0.034	0.034	0.034	169	163	169
(4) $D_W = 0.02$	0.034	0.034	0.034	169	165	173
(4) $D_W = 0.1$	0.034	0.034	0.034	168	165	192
(4) $D_W = 0.5$	0.034	0.034	0.034	163	160	241

A typical set of results is shown in Table 2 for $\lambda < \Phi$ and $\lambda > \Phi$ and for varying the relationship between D_X and D_Y or D_W. By changing the parameter values and comparing the results for many such tables it has been possible to divide the results into separate categories based on the wave speed and position of the leading edge (see cases 1–4 below). (Note: Although Table 2 contains results for specific parameters Figs 2–5 are presented for generalised time and distance to highlight the generality of the spatial patterns produced.)

General results for this study are that whenever $\lambda < \Phi$ (equating to pathogen extinction in the non-spatial set-up) a travelling wave of disease will not occur (White et al. 1999). When $\lambda > \Phi$ (implying coexistence dynamics for the host and pathogen in the non-spatial set-up), a travelling wave of disease is observed (Dwyer 1994, White et al. 1999). When a travelling wave occurs for the spatial model (eq. 1) the pattern of spread is determined by the initial conditions and the rate of spread of healthy hosts relative to infected hosts or the pathogen. The possible patterns of spread have been categorised into four separate cases.

Case 1: $\lambda < \Phi$, D_X, D_Y and $D_W > 0$

Here, inequality (3) is not satisfied, implying that in the non-spatial case the pathogen will become extinct. Similarly in the spatial case the pathogen becomes extinct at all points of the land surface, resulting in a wave of healthy hosts spreading across the spatial domain at the carrying capacity (Fig. 2). In effect, once the pathogen becomes extinct, the system of PDEs (1) can be reduced to one PDE

$$\frac{\partial X}{\partial t} = rX\left(1 - \frac{X}{K}\right) + D_X \frac{\partial^2 X}{\partial x^2}, \qquad (4)$$

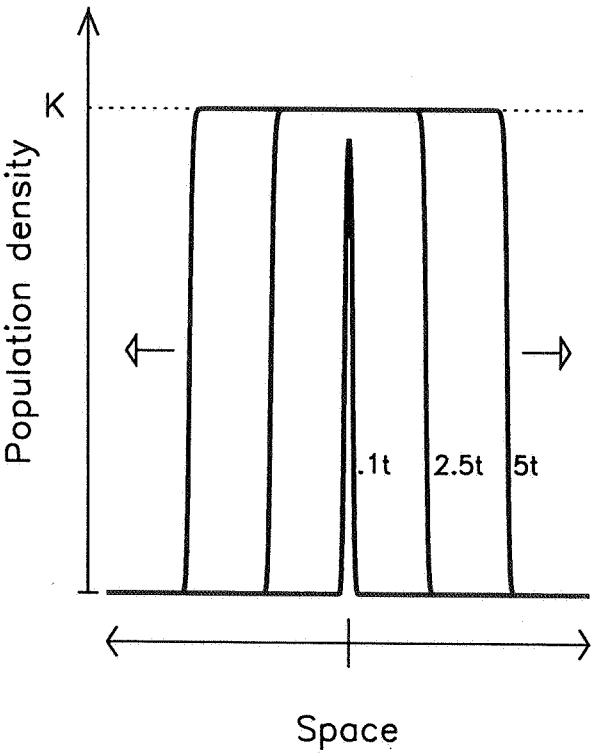

Fig. 2. The dispersal pattern for case 1 ($\lambda < \Phi$, D_X, D_Y and $D_W > 0$). Here, the disease becomes extinct at all points on the land surface and the host (solid line) can disperse at the carrying capacity density. Parameters are as in Fig. 1 with $\alpha = 0.05\ d^{-1}$, $\lambda = 1.0 \times 10^4\ d^{-1}$, $v = 1 \times 10^{-10}\ m^2\ d^{-1}$, $D_X = D_Y = D_W = 0.01\ m^2\ d^{-1}$.

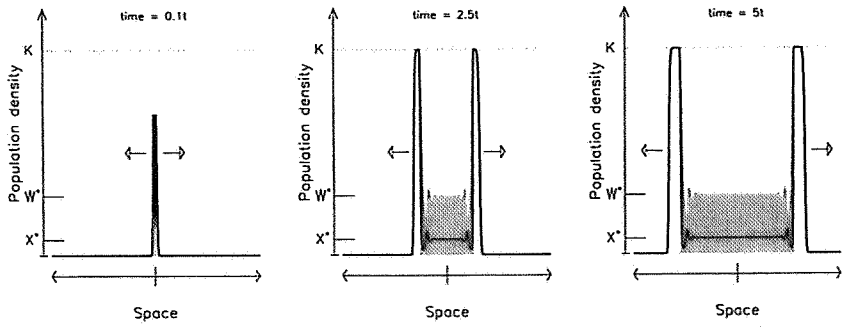

Fig. 3. The dispersal pattern for case 2 ($\lambda > \Phi$, $u_X > u_Y$ or u_W). The faster wave speed of the host (solid line) allows it to evade the pathogen (grey shaded) and disperse at the carrying capacity density. Behind the wavefront, the disease spreading at a slower rate transforms the host population from the carrying capacity to the coexistence equilibrium density, X^*. Parameters are as in Fig. 1. with $\alpha = 0.05$ d^{-1}, $\lambda = 1.0 \times 10^{-4}$ d^{-1}, $D_X = 0.01$ m^2 d^{-1}, $D_Y = 0$, $D_W = 0.002$ m^2 d^{-1}.

where $r = a - b$. The existence of travelling wave solutions converting populations from zero to that of the carrying capacity has previously been described (Fisher 1937, Murray 1989) for model formulations similar to eq. (4). The same results can be applied here. Biologically the result can be interpreted as indicating that if the pathogen is not sufficiently 'infectious' to become established at one point then it will not become established at any spatial point. This means the insect host can spread unaffected by the disease across the whole land surface. In relation to population control, this result highlights the importance of selecting a pathogen that can be sustained in the population. Since there is rarely a choice of pathogen, the chances of sustainability will depend on other factors, i.e. the pathogen is more likely to be sustained in habitats in which the host has a high carrying capacity (due to eq. 3).

Case 2: $\lambda > \Phi$, $u_X > u_Y$ or u_W

When the wave speed of the healthy hosts is greater than that of either the infected hosts or the pathogen, then at the wavefront healthy hosts can avoid contact with the disease and disperse at the carrying capacity density (Fig. 3). Behind the host wavefront a wave of disease also disperses outwards and transforms populations from the carrying capacity density to that of the coexistence equilibrium. The distance between the leading edges of healthy hosts and the disease increases with time. For parameter values as in Table 2, this pattern is estimated to occur if $D_X > 2D_Y$ or $D_X > 3.1D_W$. In terms of population control, a disease which spreads at a slower rate than its host is not desirable as it allows the pest to spread at disease-free levels over increasingly large regions of the land-surface.

Case 3: $\lambda > \Phi$, $u_X = u_Y = u_W$, $l_X > l_W$

As the diffusion coefficient of either the infected hosts or the pathogen is increased, there comes a point when all wave speeds are equal yet the leading edge of healthy hosts is still greater than that of the disease (Fig. 4). (This situation arises for $0.5D_Y < D_X < 2D_Y$, or $D_W < D_X < 3.1D_W$ for parameters as in Table 2.) At the leading edge, the density of healthy hosts peaks, since here the infection rate per host is less than in the interior of the outbreak. Nevertheless this peak is below the carrying capacity density and much 'sharper' than in case 2.

Case 4: $\lambda > \Phi$, $u_X = u_Y = u_W$, $l_X < l_W$

When the infected hosts or pathogen are considerably more mobile than the healthy hosts, (when $D_Y > 2D_X$ or $D_W > D_X$ for parameters as in Table 2) then although the wave speeds remain the same the leading edge of the pathogen extends beyond that of the host. In this situation the density of healthy hosts at the wavefront is reduced considerably below the carrying capacity (Fig. 5) (and below the values observed in case 3, Fig. 4). This occurs because the pathogen can spread beyond the host leaving no pathogen-free regions for the host to enter. In terms of population control, this set-up is desirable as the insect spread is at low levels. Note, a peak outbreak occurs at the foci immediately after introduction, due to the delay before the disease becomes fully established. This creates an isolated patch of high-density healthy hosts for an initial period. Once the disease is established, this patch is reduced to the levels of the coexistence equilibrium and the host disperses at much reduced levels.

Generality of results

The general patterns described in Figs 2–5 will occur for the whole of the model parameter space, and knowledge of which pattern will be generated can be determined from universal parameters – namely the wave speed and position of the leading edge of the host and the pathogen. However, since these universal parameters are not exclusive functions of the diffusion coefficients D_X, D_Y and D_W, some of the patterns can be generated for fixed diffusion coefficients by varying the parameters which determine the reaction kinetics in the model (i.e. the parameters contained in eq. 3). For example, with all other parameters fixed, varying the

value of v can generate cases 1 – 3 (note: the actual pattern generated is still determined by the universal parameters). Case 4 in which the leading edge of the pathogen extends beyond that of the host cannot be generated by manipulating non-spatial parameters because the reaction parameters can only increase or decrease the effectiveness of infection, and therefore rely on the availability of hosts to infect.

The generalised host-pathogen model (eq. 1) is not an accurate description of many of the forest insect species to which pathogen control strategies are applied (Bird and Elgee 1957, Bird and Birk 1961, Stairs 1965, Entwistle et al. 1983, Otvos et al. 1987a, b, Dwyer and Elkinton 1995). In particular, the behaviour of these forest insect systems is typically constrained by a seasonal environment. This implies that host-pathogen activity and host dispersal will occur for a limited period each season, and that births will occur over a short period at the start of each season rather than continuously (at least for species which exhibit one generation per season). Would the same patterns be evident in a more realistic representation of a forest insect system? To test this, eq. 1 is modified to represent a specific forest insect system; namely the winter moth, *Operophtera brumata* (L.) and its nuclear polyhedrosis virus. This modelling strategy will provide invaluable information about the type of behaviour possible in this system as well as being used to test the generality of the dispersal patterns to model formulation.

The patterns of dispersal of winter moth have been noted to differ on different plant species. In oak forests winter moth spread occurs at high density across the whole forest, whereas in Sitka spruce winter moth outbreaks are constrained to isolated patches (Watt pers. comm.). It may be possible to explain these patterns by different dispersal regimes in the different plant types.

Modelling winter moth dynamics

Winter moths are dependent on a seasonal environment (Varley et al. 1973) and this can be represented by a two-stage model (see Briggs and Godfray (1996) for a two-stage model of temporal seasonal dynamics and White et al. (1999) for an extension to spatial systems).

The first stage, modelled using continuous dynamics, represents the period in which the insect larvae and pathogen can interact. The second stage will represent the period from larval pupation until larval emergence in the following season. A discrete mapping will be used to represent this 'between season' behaviour for the host since during this period host pathogen interactions do not occur. Pathogen dispersal will continue during this period. The dispersal of the host is more complicated. In winter moth, adult females are flightless and tend to deposit eggs on the nearest tree following pupation. Larvae emerge on these trees and will remain there provided there are adequate food resources. If food is scarce they will balloon and become airborne in search of resources. The model does not explicitly describe food resources, so we assume that dispersal of the host will be represented by a Gaussian (normal) distribution applied to each point on the land surface immediately prior to the next within season stage.

Stage 1: Within season

$$\frac{\partial X}{\partial t} = -bX - vXW$$

$$\frac{\partial Y}{\partial t} = vXW - (b + \alpha)Y$$

$$\frac{\partial W}{\partial t} = \lambda Y - (\mu + v(X + Y))W + D_W \frac{\partial^2 W}{\partial x^2}. \qquad (5)$$

Here, parameters are as defined earlier. The birth and diffusion terms are omitted from the host classes, as they are assumed to occur at the beginning of the season and therefore represented in stage 2.

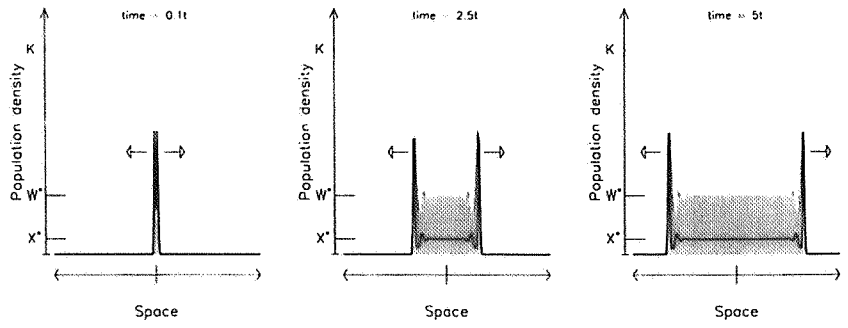

Fig. 4. The dispersal pattern for case 3 ($\lambda > \Phi$, $u_X = u_Y = u_W$, $l_X > l_W$). The host and pathogen disperse at the same speed, but the leading edge of the host extends beyond that of the pathogen. At the leading edge the host density peaks, although at a density less than the carrying capacity, and behind this peak the density is transformed to that of the coexistence equilibrium, X^*. Parameters are as in Fig. 3, except $D_W = 0.008$ m^2 d^{-1}.

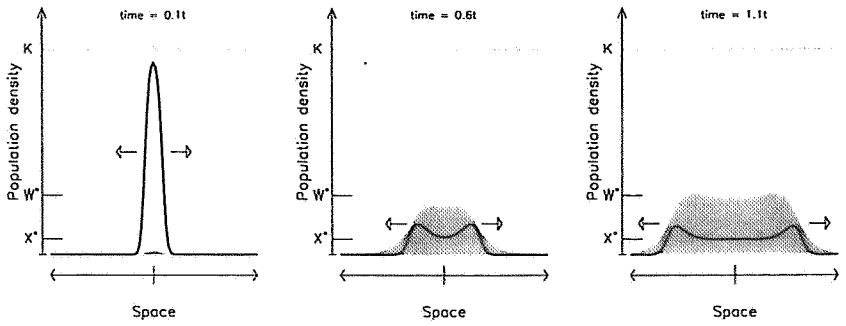

Fig. 5. The dispersal pattern for case 4 ($\lambda > \Phi$, $u_X = u_Y = u_W$, $l_X < l_W$). The host and pathogen disperse at the same rate, but the leading edge of the pathogen extends beyond that of the host. There are no pathogen-free regions for the host to encroach, and the density at the leading edge is considerably reduced. Note, that there is initially a patch of high-density healthy hosts caused by the delay before the pathogen becomes fully established. Parameters are as in Fig. 3, except $D_W = 0.05$ m^2 d^{-1}.

Stage 2: Between seasons

A discrete mapping is used to transform the density of healthy hosts at the end of the larval stage to that at the beginning of the next season when larvae emerge. Thus,

$$X_{start} = 0.5 X_{end}\, s_{la} f_a\, s_{el}. \tag{6}$$

Here, X_{end} and X_{start} represent the density of larvae at the end of a season and the beginning of the following season, respectively. The parameter s_{la} represents the proportion of healthy hosts that survive from larvae to adult (effectively pupal survival); f_a is the fecundity of adults and s_{el} is the proportion of healthy hosts that survive from egg to healthy larvae (the 0.5 assumes an equal number of male and females become adults). These parameters are derived from Varley et al. (1973) as follows:

The pupal survival rate can be calculated from the sum of two k-values ($k_5 = 0.35 \log_{10} X$, and $k_6 \approx 0.17$) where k-values relate to survival rates, s, as $s = 10^{-k}$. Thus,

$$s_{la} = 10^{-0.35 \log_{10} X_{end}} 10^{-0.17} = 0.7 X_{end}^{-0.35}. \tag{7}$$

Female winter moths are reported to contain on average 150 eggs, thus $f_a = 150$. The survival from egg to larvae (known as winter disappearance by Varley et al. (1973)) is also described by a k-value, producing an average $s_{el} = 0.15$. Varley et al. (1973) report large variation in s_{el} but we choose to fix its value to enable the spatial patterns of disease spread to be observed clearly. Tests have been undertaken with a stochastic representation of this parameter, giving a good representation of the variability observed in natural winter moth populations. It did not alter the general spatial behaviour or the qualitative shape of the dispersal patterns described below.

Over the same period the infected host and pathogen classes are represented by the following equations:

$$\frac{\partial Y}{\partial t} = -(b+\alpha)Y$$

$$\frac{\partial W}{\partial t} = \lambda Y - \mu W + D_W \frac{\partial^2 W}{\partial x^2}. \tag{8}$$

Here, any infected larvae present at the end of the season are assumed to die and lyse (infected larvae die on average in a $(b+\alpha)^{-1}$ time period), thereby releasing pathogen particles. It is assumed that all infected larvae die before the beginning of the next season. The pathogen continues to decay and disperse between seasons.

Immediately after host emergence, healthy hosts disperse according to a Gaussian distribution. Thus, for each land point x_i dispersal is represented as follows:

$$X_{start}(x_i) = \sum_{j=0,n} X_{start}(x_j) \frac{1}{D_s\sqrt{2\pi}} \exp -\frac{(x_i - x_j)^2}{2D_s^2}. \tag{9}$$

Numerical analysis of the temporal dynamics of the model for winter moth can be divided into four parameter-dependent types of behaviour: pathogen extinction; and equilibrium, cycles and chaos in host and pathogen density (Fig. 6). A wave of disease does not occur for parameters that produce pathogen extinction (as in case 1 of the general model, eq. 1). For parameters that produce coexistence behaviour a wave of disease will develop and the patterns of dispersal can be categorised by the wave speed and the position of the leading edge (as in cases 2–4 of the general model).

Thus, the same patterns, partitioned by the same universal parameters, are produced by the specific and general host-pathogen models. Tests using additional model set-ups suggest that these patterns of dispersal (cases 1–4) are robust to model formulation provided the following criteria are satisfied for the non-spatial (reaction only) part of the model. These being that in the absence of the disease, the host is constrained by a finite limit (e.g. the carrying capacity for the general model), and that when the disease is influential, dynamics that allow the host and pathogen to coexist are produced (i.e. host and pathogen equilibria, cycles or

chaos). (Note: the nature of the coexistence dynamics does not qualitatively alter the patterns reported, but does affect the dynamic in the wavetrain. For example, for parameters that produce stable cycles in the non-spatial model, the behaviour in the wavetrain would also cycle (Murray 1989), rather than tend to an equilibrium as in Figs 2–5.)

Discussion

The results from a simple, spatial host-pathogen model produce four distinct spatial patterns which can be categorised by the strength of interaction between the host and the disease and by comparing the wave speed and the position of the leading edge of the host and the pathogen. This study introduces the possibility of disease spread by pathogen-bearing agents, achieved by including a diffusion term for the pathogen, D_H. Previously dispersal had been represented by diffusion terms for healthy and infected hosts only, D_X and D_Y, respectively (Dwyer 1992, 1994, Dwyer and Elkinton 1995, White et al. 1999). The results show that including pathogen dispersal did not alter the range of dynamic possibilities, because the reported behaviour can be exhibited by varying either D_Y or D_H relative to D_X. This study suggests that the role of pathogen-bearing agents may nevertheless be crucial, since the rate of dispersal of such agents (which includes dispersal by adult hosts, predators and parasites) is likely to be greater than that of host larvae, and a faster rate of disease spread is key to effective population control. When direct pathogen dispersal is excluded, effective population control requires infected hosts to disperse at a greater rate than healthy larvae. One may intuitively expect the converse to be true, since infection will inevitably kill the host. However, Vasconcelos et al. (1996) reported that infected hosts of *Mamestra brassicae* are more active (during the mid-infection period) than their healthy counterparts, with the range of dispersal increased three- to five-fold. Thus, larval dispersal may be an equally crucial dispersal mechanism.

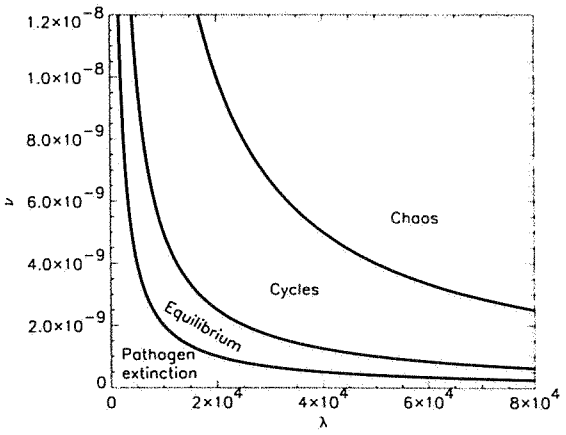

Fig. 6. The r-λ parameter space portrait detailing where the different dynamic behaviour occurs for the model of winter moth. The parameters which are not detailed in the main text, are $\alpha = 0.05$ d^{-1}, $b = 0$, $\mu = 0.01$ d^{-1}, $D_X = D_H = 0$. The boundaries between regions are calculated by numerical simulations, and are therefore approximate.

The results indicate that the disease will disperse as a single wave, thereby extending previous findings for host movement (Dwyer 1994, White et al. 1999), to include explicit pathogen dispersal. Comparisons with empirical studies examining the effects of pathogens on insect pests (Bird and Elgee 1957, Bird and Birk 1961, Stairs 1965, Young 1974, Shepherd et al. 1984, Otvos et al. 1987a, b) are difficult as they lack detailed descriptions of the patterns of dispersal (although arguments suggesting wave-like disease spread are often suggested). Exceptions to this are the studies of Entwistle et al. (1983) and Dwyer and Elkinton (1995), who present detailed descriptions of the wave-like disease dispersal patterns. Both general and specific reaction-diffusion models have been compared to these studies, enhancing our understanding of the processes driving disease dispersal (Dwyer 1994, Dwyer and Elkinton 1995, White et al. 1999). The results from these models (which have included host dispersal only) correspond well with those observed by Entwistle et al. (1983). Findings reported in the study presented here indicate that these patterns of spread could equally be attributed to explicit disease dispersal (by pathogen-bearing agents). In fact, the hypothesis of Entwistle et al. (1983) that pathogen-bearing agents may be responsible for disease spread is supported by this study.

Comparisons between the results presented here and those observed in experimental and theoretical studies of host-parasitoid interactions (Brodmann et al. 1997, Hastings et al. 1997) can also be drawn. Field observations indicate that the highest population density of the host occurs at the edge of an outbreak, and this is verified by qualitative results from a general model. Hastings et al. (1997) suggest such a pattern will occur whenever the parasitoid has high mobility compared to the host, and question whether this pattern is observable in other systems. The results presented here display the same phenomena, but suggest that host density will be greatest at the edge of the outbreak whenever the host disperses from a single focus and is influenced by the disease regardless of the relative speed of host and disease spread (i.e. cases 2–4).

The results also indicate that the long-term wave speed of the disease (u_Y or u_H) cannot exceed that of the host (u_X), regardless of the size of the infected host or pathogen diffusion coefficient. This has been tested numerically, and can be understood biologically. Pathogen replication relies on host infection, so the pathogen requires contact with susceptible hosts to survive. If the pathogen disperses to far away from the host it will

decay before it can infect, thereby constraining the speed of disease spread. This explains why our results also apply when the pathogen is introduced across the entire land surface as well as at one point. Here pathogen distributed away from the host will decay before producing infection, leading to the same long-term dynamics as reported in cases 1–4. This suggests that 'blanket' spraying of a pathogen may not be sufficient to prevent high-density pest outbreaks.

The results from a simple, spatial model of host-pathogen interactions have been shown to generalise to more specific descriptions of forest insect systems by developing a model of winter moth and its NPV. Could the spatial host-pathogen interactions be responsible for controlling the spread of winter moth in natural systems? In oak forests it has been noted that winter moth spread occurs at high density across the whole forest, whereas in Sitka spruce winter moth outbreaks are constrained to isolated patches (Watt pers. comm.). Such patterns are reflected by the model results when the relative mobility of the host and pathogen are different (i.e. cases 2 and 4), implying that the observed patterns could be produced if the rates of dispersal are different on the two tree species. Recall also, that the dispersal patterns can be altered by varying the rate of transmission (or infectivity) of the disease, r, for fixed dispersal parameters, suggesting that differences in pathogen infectivity on different plants may also influence the dispersal pattern. Such differences have been shown to exist for gypsy moth-virus systems (Foster et al. 1992, Appel and Schultz 1994), where tannin levels markedly influence the effectiveness of the pathogen. Thus, the spatial interaction of host and pathogen coupled with the strength of the infection of the pathogen can play a crucial role in determining the patterns of forest insect outbreaks and indeed may explain the patterns observed in winter moth. Without detailed field results it is difficult to judge whether host-disease interactions alone could produce the dispersal patterns in winter moth. Field studies are currently being undertaken to assess the relative roles of disease, infection and other factors in controlling the spread of winter moth outbreaks (Hails pers. comm.), with the results presented here used to construct specific field experiments. Verification of the findings will have important consequences for the use of free-living pathogens as a method of controlling insect pests.

Acknowledgements This work is supported by the Centre for Ecology and Hydrology Integrating Fund.

References

Anderson, R. M. and May, R. M. 1981. The population dynamics of microparasites and their invertebrate hosts. – Philos. Trans. R. Soc. Lond. B 291: 452–524.

Appel, H. M. and Schultz, J. C. 1994. Oak tannins reduce effectiveness of thuricide (*Bacillus thuringiensis*) in gypsy-moth (Lepidoptera, Lymantriidae). – J. Econ. Entomol. 87: 1736–1742.

Bird, F. T. and Elgee, D. E. 1957. A virus disease and introduced parasites as factors controlling the European spruce sawfly, *Diprion hercyniae* (Htg.), in central New Brunswick. – Can. Entomol. 89: 371–378.

Bird, F. T. and Birk, J. M. 1961. Artificially disseminated virus as a factor controlling the European spruce sawfly, *Diprion hercyniae* (Htg.) in the absence of introduced parasites. – Can. Entomol. 93: 228–238.

Bowers, R. G., Begon, M. and Hodgkinson, D. E. 1993. Host-pathogen populations cycles in forest insect? Lessons from simple models reconsidered. – Oikos 67: 529–538.

Briggs, C. J. and Godfray, H. C. J. 1996. The dynamics of insect-pathogen interactions in seasonal environments. – Theor. Popul. Biol. 50: 149–177.

Brodmann, P. A., Wilcox, C. V. and Harrison, S. 1997. Mobile parasitoids may restrict the spatial spread of an insect outbreak. – J. Anim. Ecol. 66: 65–72.

Dwyer, G. 1992. On the spatial spread of insect pathogens: theory and experiment. – Ecology 73: 479–494.

Dwyer, G. 1994. Density dependence and spatial structure in the dynamics of insect pathogens. – Am. Nat. 143: 533–562.

Dwyer, G. and Elkinton, J. S. 1995. Host dispersal and the spatial spread of insect pathogens. – Ecology 76: 1262–1275.

Entwistle, P. F., Adams, P. H. W., Evans, H. F. and Rivers, C. F. 1983. Epizootiology of a nuclear polyhedrosis virus (baculoviridae) in European spruce sawfly (*Gilpinia hercyniae*): spread of disease from small epicentre in comparison with spread of baculovirus disease in other hosts. – J. Appl. Ecol. 20: 473–487.

Fisher, R. A. 1937. The wave of advance of advantageous genes. – Ann. Eugenics 7: 353–369.

Foster, M. A., Schultz, J. C. and Hunter, M. A. 1992. Modelling gypsy moth-virus-leaf chemistry interactions: implications of plant quality for pest and pathogen dynamics. – J. Anim. Ecol. 61: 509–520.

Hastings, A., Harrison, S. and McCann, K. 1997. Unexpected spatial patterns in an insect outbreak match a predator diffusion model. – Proc. R. Soc. Lond. B 264: 1837–1840.

Murray, J. D. 1989. Mathematical biology. – Springer-Verlag, Berlin.

Otvos, I. S., Cunningham, J. C. and Friskie, L. M. 1987a. Aerial application of nuclear polyhedrosis virus against Douglas-fir tussock moth, *Orgyia psuedotugata* (McDunnough) (Lepidoptera: Lymantriidae). I. Impacts in the year of application. – Can. Entomol. 119: 697–706.

Otvos, I. S., Cunningham, J. C. and Alfaro, R. I. 1987b. Aerial applications of nuclear polyhedrosis virus against Douglas-fir tussock moth, *Orgyia psuedotugata* (McDunnough) (Lepidoptera: Lymantriidae). II. Impacts 1 and 2 years after application. – Can. Entomol. 119: 707–715.

Shepherd, R. F., Otvos, I. S., Chorney, R. J. and Cunningham, J. C. 1984. Pest management of the Douglas-fir tussock moth (Lepidoptera: Lymantriidae): prevention of an outbreak through early treatment with a nuclear polyhedrosis virus by ground and aerial applications. – Can. Entomol. 116: 1533–1542.

Stairs, G. R. 1965. Artificial initiation of virus epizootics in forest tent caterpillar populations. – Can. Entomol. 97: 1059–1062.

Varley, G. C., Gradwell, G. R. and Hassell, M. P. 1973. Insect population ecology. – Blackwell Scientific, Oxford.

Vasconcelos, S. D., Cory, J. S., Wilson, K. R. et al. 1996. Modified behaviour in Baculovirus-infected lepidopteran larvae and its impacts on the spatial distribution of inoculum. – Biol. Control. 7: 299–306.

White, A., Bowers, R. G. and Begon, M. 1999. The spread of infection in seasonal insect-pathogen systems. – Oikos 85: 487–498.

Young, E. C. 1974. The epizootiology of two pathogens of the coconut palm rhinoceros beetle. – J. Invertebr. Pathol. 24: 82–92.